

Interpretation of laser scanner 3D data used to determine circular failure surface of shallow landslides

Oppikofer, T., Jaboyedoff, M., Baillifard, F., Pedrazzini, A. and Travelletti, J.

University of Lausanne, Institute of Geomatics and Analysis of Risk (IGAR), Amphipole, CH-1015 Lausanne, Switzerland, email: Michel.Jaboyedoff@unil.ch

1. Introduction

In Switzerland the landscapes have been greatly remodelled during the last glaciation period. Important quantities of glacial and fluvial sediments were deposited during the glacial retreat after the Last Glacial Maximum 17'000 years BP (Hinderer, 2001). In the region of Lausanne, South-western Switzerland, the glaciers left behind morainic sediments (Rhodanian moraine) and fluvio-glacial sediments that cover the underlying fluvial and marine sandstones of the Molasse basin. Glacier lakes formed in many of the topographic depressions, which were filled by varved sediments (clayey or sandy silts). In the vicinity of the study site, these silts are up to 25 m thick and were deposited during the Dryas I period ($13'219 \pm 180$ years BP (Gabus et al., 1987)). These sediments are typical for a late glacial climate.

The Sorge River, a secondary tributary to the Lake of Geneva, incises these silt formations. As the region of Lausanne is densely populated and constructed, the river course is restrained due to channelling. Active bank erosion is observed at many places. This erosive process becomes especially important during and after heavy rainfalls. In order to mitigate this problem, remediation works were carried out on a 150 m long section between spring and autumn 2005 (Figure 1). The river bed was enlarged (from between 3 and 7 m to between 5 to 11 m) and its banks were smoothed (3 to 4 m high banks with a slope angle of about 25°). In narrow and in sinuous sections, stone walls (up to 2.5 m in height) were constructed to stabilize the slope. In this renaturalized section, the river gradient is between 80 and 90 cm per 100 m.



Figure 1: Views of the Sorge River to the West (taken on March 16th 2006). The point cloud of the laser scanner and the photograph show the area of the remedial works that were done in 2005. The scar of the first landslide is also shown.

Two heavy rainfall events in March and April 2006 lead to a rapid increase of the river flow rate. The precipitations from 8th to 10th of April 2006 caused the rise of the water table of approximately 90 cm. The increased energy of the Sorge River probably leads to intense bank

erosion, where no stone protection walls were built. This erosion induced landslides within the river's banks.

In this study we use 3D laser scanner data to follow the evolution of the Sorge River banks. The main goal of this study is to follow the movements of landslides occurring on the river's flanks. Morphologic considerations, combined to geometric and mechanical models will improve the understanding of such rotational slides.

Here we present some preliminary results on the interpretation of laser scanner data on two small-scale landslides.

2. Methods

The study site is the whole, 150 m long section of the Sorge River, where remediation works were conducted in 2005.

Two scan campaigns were performed on March 16th 2006 and April 12th 2006 with an Optech ILRIS 3D laser scanner. During the first campaign the whole section was scanned. One landslide on the left, northern flank already occurred before this reference scan. The second acquisition was carried out after the heavy rainfalls from 8th to 10th of April 2006. The newly appeared landslides were scanned in detail. On the left flank, two new landslides happened in the meantime. On the right, southern flank, several minor landslides were also found.

The point clouds of the laser scans of the pre-existing and one of the new landslides were treated and interpreted using the PolyWorks[®] software from InnovMetric Software Inc.

3. Results

3.1. First landslide

The first landslide occurred before March 16th 2006. The scar of this landslide is perfectly circular and has a maximal height of 1.3 m. The body of the landslide shows a typical morphology of a rotational landslide with a planar landslide head and an accumulation of soil material in the foot part (Figure 2).

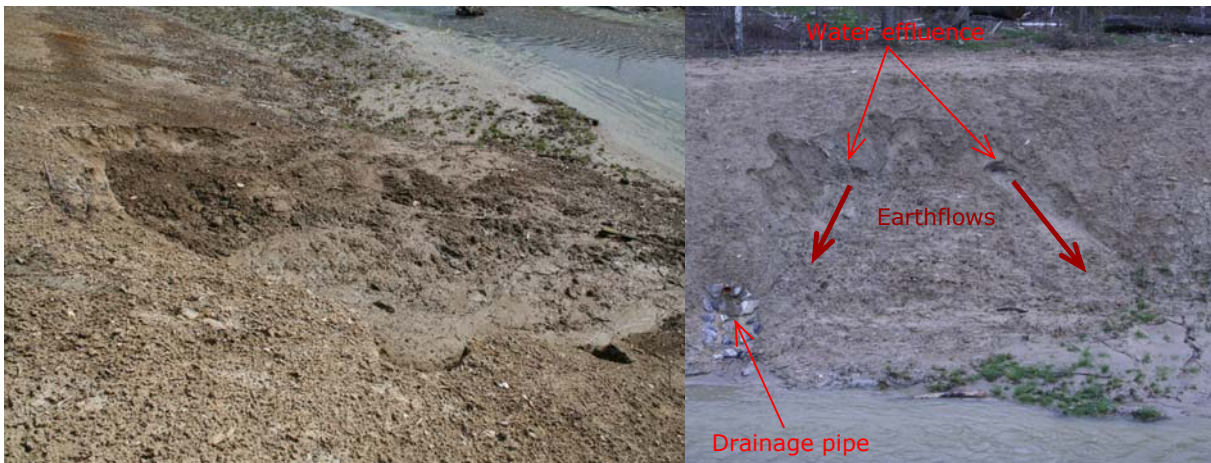


Figure 2: Photographs of the pre-existing landslide (left: taken on March 16th 2006; right: taken on April 12th 2006). The circular failure surface, the landslide's head and foot are visible. The main body of the slide is wet, indicating arrival of groundwater. Water effluences are observable on the picture taken on April 12th 2006. They probably caused some small earthflows.

The data were compared to a primitive plane fitted with the non-dislocated points of the flank. The error map between the point cloud and the plane (Figure 3) clearly shows the scar area and the head of the slide (negative differences, up to -0.8 m), as well as the foot of the earth slide (positive differences, up to $+0.4$ m). Several minor circular landslides developed all around the main scar. The missing volume in the head area is more important than the one deposited in the foot of the slide. It seems that a part of the material was eroded during the high water level stage.

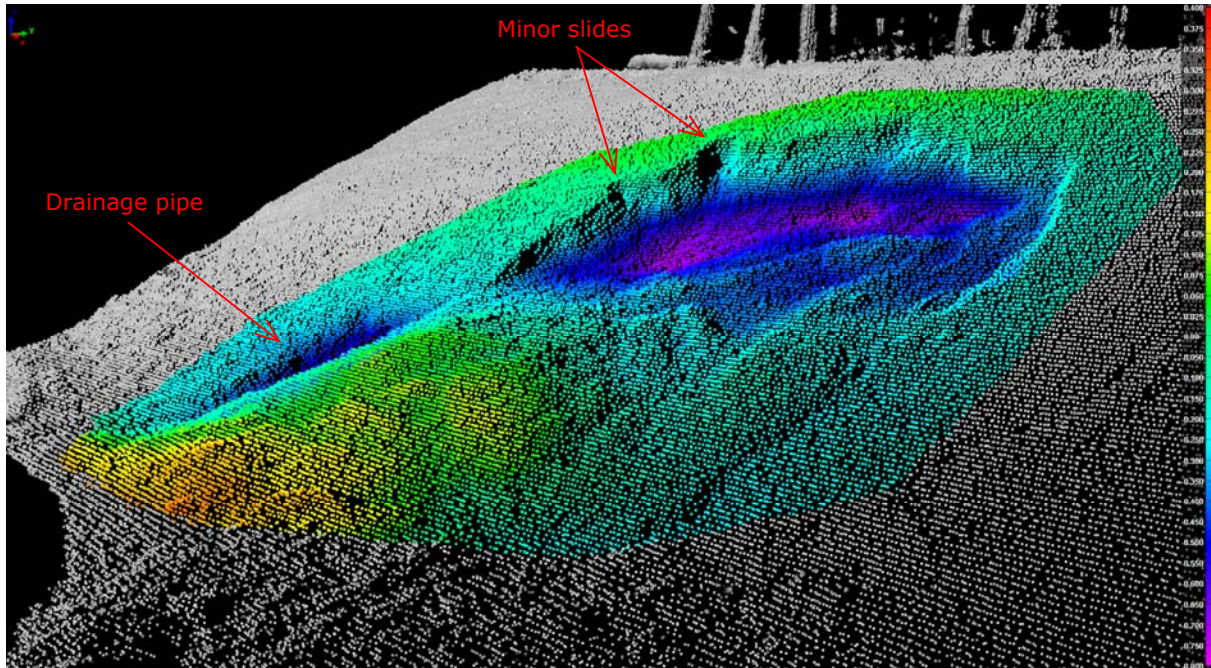


Figure 3: Comparison (error map) of the reference point cloud (acquired on March 16th 2006) with a primitive plane corresponding to the initial bank surface (view to the NW). The colours indicate the shortest distance between the point and the plane. Positive differences (green to red colours: 0 m to $+0.4$ m) correspond to the foot of the slide, whilst the negative differences (light blue to violet colours: 0 m to -0.8 m) correspond to the scar area and the head of the slide. The Sorge River flows in the lower left corner. The depression next to the foot of the slide is due to the drainage pipe visible in Figure 2.

The differences between the scans of the two campaigns reveal only small movements between the March 16th and the April 12th 2006 (Figure 4). Some parts of the main scar slid further downwards. Water effluences at two spots could also be identified. They initiated small earthflows that could be followed downwards. The main track of both earthflows, as well as the depositional area of the right flow could be delimited. The foot of the main slide got slightly eroded during the April 2006 flooding.

A vertical cross section through the central part of the slide confirms the rotational sliding mechanism (Figure 5). A sphere can be fitted through the points of the main scar. Its radius is 6.3 m and its centre lays about 5.5 m above the pre-failure surface.

Knowing the angle between the initial surface and the landslide head (α) and the distance between the top of the scar and the top of the sliding mass (l), it is possible to calculate the radius (R) of the circular failure surface by:

$$R = \frac{l}{2 \sin(\alpha/2)}$$

For the first landslide a radius of 6.5 m has been calculated with $\alpha = 10.2^\circ$ and $l = 1.15$ m. This value corresponds well to the radius of the sphere calculated with a best fit ($R = 6.3$ m).

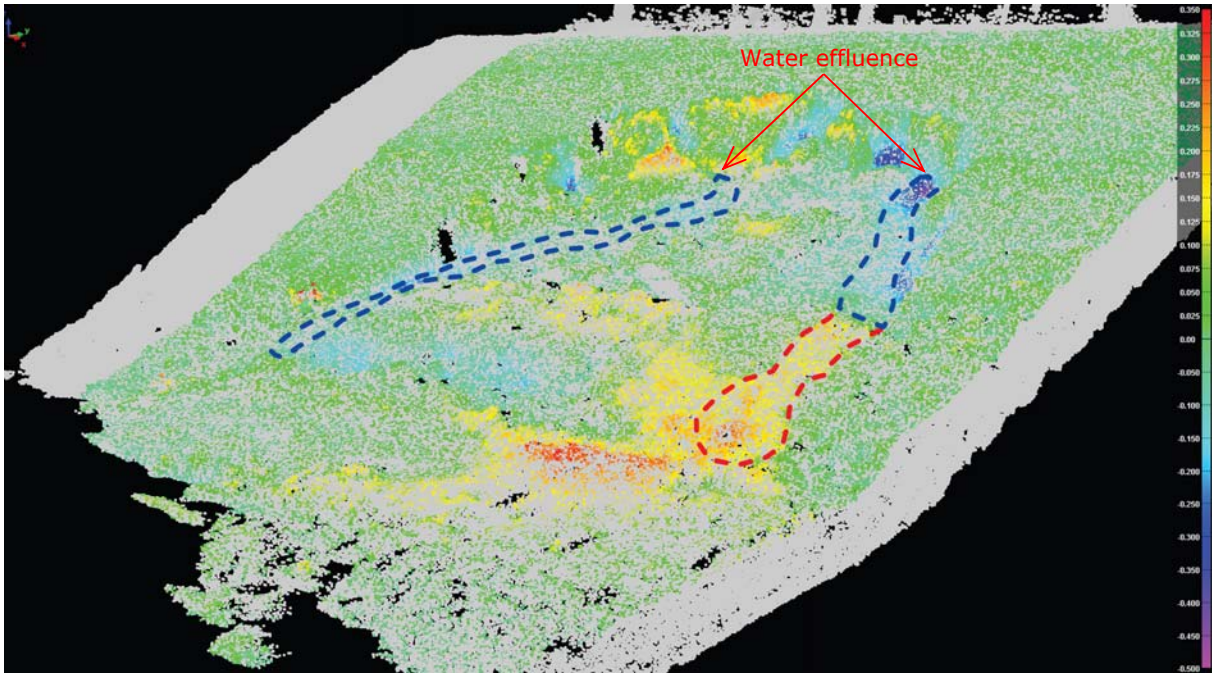


Figure 4: Differences (error map) between the two point clouds (acquired on March 16th and April 12th 2006). The colours indicate the vertical distance between the points of the two scans. Positive differences (green to red colours: 0 m to +0.35 m) correspond to the foot of the main slide, the feet of some minor slides in the scar area and the deposit area of the earthflow. Negative differences (light blue to violet colours: 0 m to -0.5 m) correspond to the scar area of the minor slides, as well as the source area and main tracks of the earthflows. The dashed contours indicate the main tracks of the earthflows (in blue) and the deposit area (in red). The view is towards the NW with the Sorge River flowing in the lower left corner.

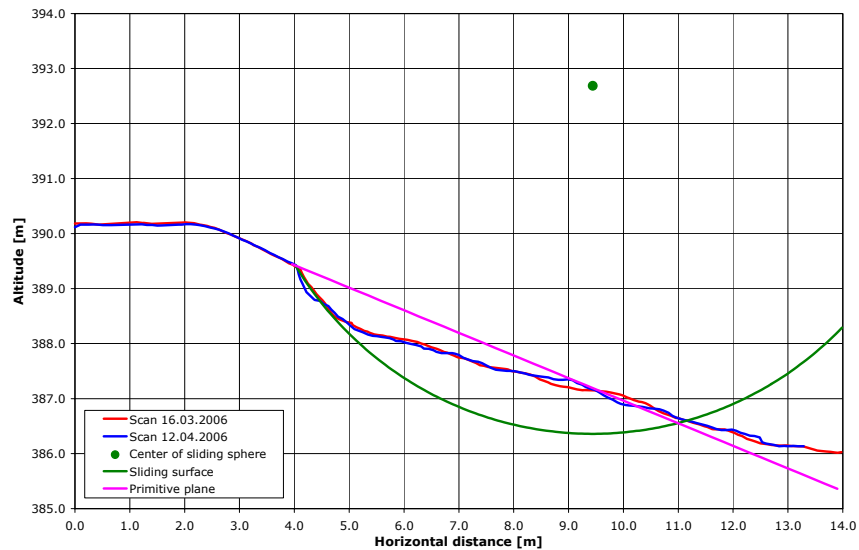


Figure 5: Cross section through the first landslide. The differences between the two scans (red: March 16th 2006; blue: April 12th 2006) are caused by the minor slides in the scar area and the earthflows. The trace of the primitive plane corresponding to the initial surface (in pink) is shown. The best-fit sphere and its centre (in green) represent the sliding surface and the rotation axis.

3.2. Second landslide

The second landslide in the eastern part of the study area occurred in the period between the two scanning campaigns (Figure 6). It was probably caused by the intense rainfall event of 8th to 10th April 2006 and the increased river flow rate. The landslide is composed of a main rotational slide and a smaller secondary rotational slide. Small scarps are also observable on both sides of the landslide. The main scarp is circular and reaches a height of 0.6 m in the central part. The lateral extent of the landslide is approximately 5.5 m. Apparently, the landslide initiated already during the flooding of 8th to 10th of April 2006, but displacements continued after the decrease of the river's water table (Figure 6).



Figure 6: Photographs of the second landslide (left: taken on 10th of April 2006 during the flooding; right: situation on April 12th 2006). The main scarp (red), the secondary scarp (orange) and the minor scarps (yellow) are discernable on both pictures. The landslide continued its rotational movement in the interval of the two pictures.

The differences between the two scans directly reveal the total displacement of the landslide (Figure 7). Negative differences in the scar area attain 0.6 m. At the foot of the slide the accumulated materials caused positive altitude differences of up to 0.4 m. The overall geometry and morphology of the landslide suggest that the main slide (dashed red line in Figure 6 and Figure 7) occurred before the secondary slide (orange line). The minor scarps (yellow lines) are probably caused by the displacement of the main body which destabilized the entire slope.

The cross section through the main part of the second landslide (Figure 8) shows a nice example of a rotational slide. The initially planar surface was rotated around an axis perpendicular to the cross section. The sliding surface is modelled with a sphere inscribed in the scar area. It has a radius of 2.5 m and a centre point, corresponding to the rotation axis, situated approximately 1.5 m above the river bank.

The radius determined on the basis of the mean distance between top of the scar and the top of the moved mass ($l = 0.50$ m) and the angle between the initial and rotated surface ($\alpha = 11.5^\circ$) is 2.45 m. This value is in good agreement with the radius of the best-fit sphere ($R = 2.5$ m).

4. Conclusions and perspectives

Sequential laser scan images are a powerful tool to understand the geometry, the morphology and finally the mechanism of rotational landslides. Even small changes can be followed precisely, allowing the delimitation of small movements associated to a large landslide phenomenon.

The evolution of the banks of the Sorge River will be followed with further scans. New earth slides appear almost after every heavy precipitation event. Several new landslides have been observed since the last scanning campaign. At present the slopes start to get vegetated. It will be interesting to see, if the vegetation avoids further landsliding or not.

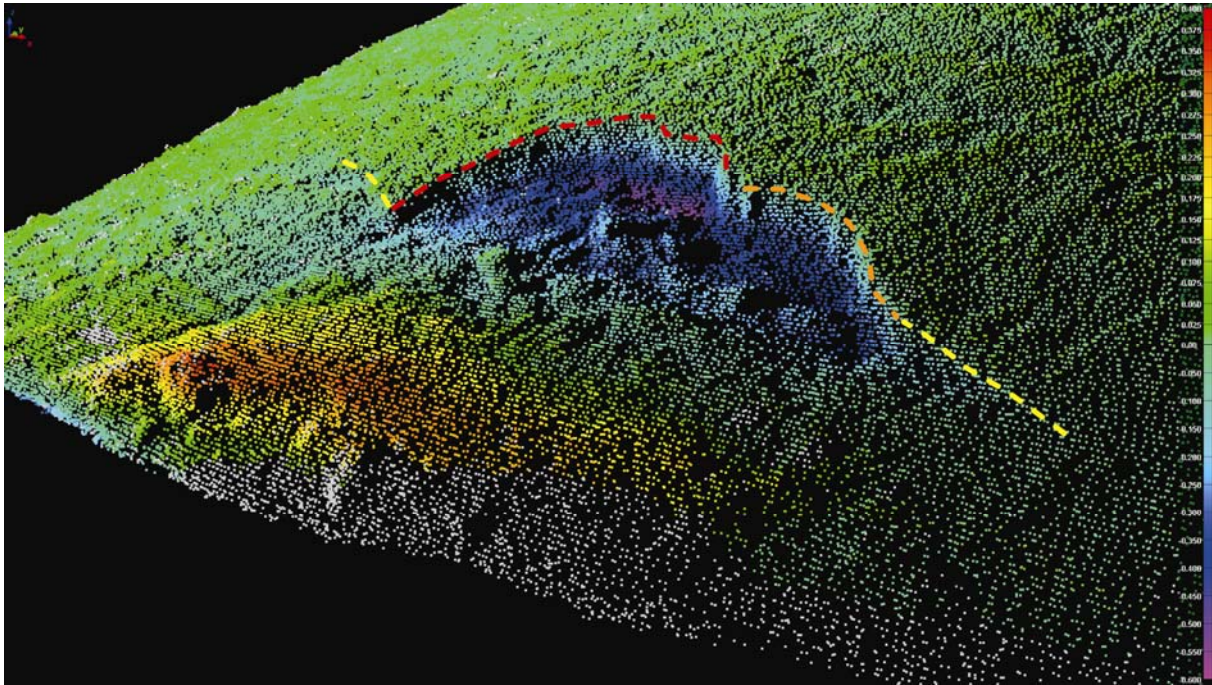


Figure 7: Error map showing the differences in altitude (z) between the point clouds of March 16th and April 12th 2006. The main and secondary rotational landslides are clearly visible (red and orange dashed lines). The small lateral scarps (yellow dashed lines) also show some displacement. The head of the main body (light blue to violet colours: 0 m to -0.6 m) and the foot of the landslide (green to red colours: 0 m to $+0.4$ m) can be identified. The view is towards the NNW with the Sorge River flowing in the lower left corner.

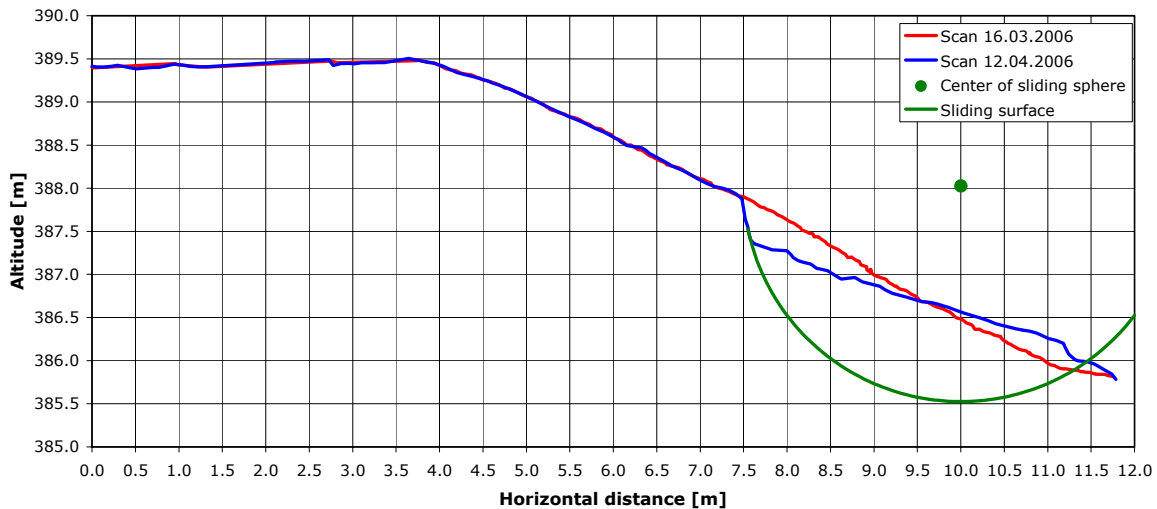


Figure 8: Cross section through the second landslide. The scan made on March 16th 2006 shows no traces of potential landsliding (red line). The scan of April 12th 2006 (blue line) shows the rotational displacement of the initial planar surface. The trace and centre of the sphere (in green) is fitted using the points of the main scar and represents the sliding surface.

Further investigations on the landslides will comprise mechanical tests, like shear resistance (vane tester) and penetration resistance (dynamic penetrometer) of the soil. Boreholes and trenches, using a hand auger and a shovel, will permit to see the sliding surface and to characterize it mechanically and materially.

Geometrical modelling will also be performed to verify the stability of the rotational landslides. Safety factors (F) will be calculated using the slice method in 2D (Bishop, 1955) and in 3D (Hungr, 1987 and Hungr et al., 1989), as well as other methods. The sloping local base level concept (Jaboyedoff and Derron, 2005) will be applied to determine the basal failure surface of the landslides.

References

- Bishop, A. W. (1955). The use of the slip circle in the stability analysis of slopes. *Géotechnique* 5, No. 1, 7-17.
- Gabus, J.-H., Lemdal, G. and Weidmann, M. (1987). Sur l'âge des terrasses lémaniques au SW de Lausanne. *Bulletin Société vaudoise de Sciences naturelles* 78/4 (372), 419-429.
- Hinderer, M. (2001). Late Quaternary denudation of the Alps, valley and lake fillings and modern river loads. *Geodinamica Acta*, 14, 231-263.
- Hungr, O. (1987). An extension of Bishop's simplified method of slope stability analysis to three dimensions. *Géotechnique* 37, No. 1, 113-117.
- Hungr, O., Salgado, F. M. and Byrne, P. M. (1989). Evaluation of a three-dimensional method of slope stability analysis. *Canadian Geotechnical Journal* 26, 679-689.
- Jaboyedoff, M. and Derron, M.-H. (2005). A new method to estimate the infilling of alluvial sediment of glacial valleys using a sloping local base level. *Geografia Fisica e Dinamica Quaternaria*, 28 (2005), 37-46.
- Weidmann, M. (1988). Atlas géologique de la Suisse 1:25000, feuille 1243 Lausanne, carte géologique et notice explicative. Service hydrologique et géologique national, Bern, Switzerland.